

Supporting Information

for

Modes of hurricane activity variability in the Eastern Pacific: implications for the 2016 season

Julien Boucharel^{1*}, Fei-Fei Jin^{2,3}, Matthew H. England¹, and I.I. Lin⁴

¹ *ARC Centre of Excellence for Climate System Science, University of New South Wales, Sydney, New South Wales, Australia*

² *Department of Atmospheric Sciences, SOEST, University of Hawaii at Manoa, Honolulu, Hawaii, USA*

³ *Laboratory for Climate Studies, Beijing Climate Center, Chinese Meteorological Agency, Beijing, China*

⁴ *Department of Atmospheric Sciences, National Taiwan University, Taipei 10617, Taiwan*

To be submitted to Geophysical Research Letters

Figure S1, S2

* Corresponding author address: ARC Centre of Excellence for Climate System Science, University of New South Wales, Sydney, NSW 2052, Australia. E-mail: j.boucharel@unsw.edu.au

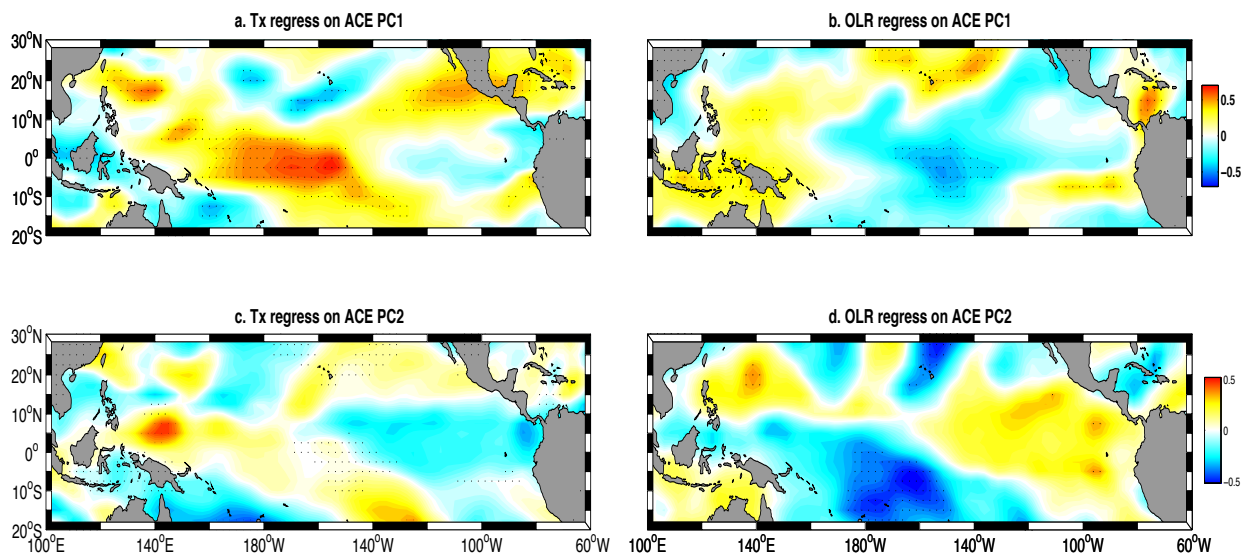


Figure S1. Lag-regression patterns of intraseasonal anomalies of surface wind stress (a. and c.) and outgoing longwave radiation (OLR, b. and d.) averaged in boreal winter and spring (January-March) onto the ACE Principal Components (PCs). The PC time series are yearly averages: early hurricane boreal season, June-September for PC2 and late season, August-November for PC1. The intraseasonal anomalies are simply calculated as follows; we remove the ENSO timescales (i.e. the regressed Nino3.4 index) from the interannual anomalies relative to a monthly mean climatology. OLR data come from NOAA-NCEP [*Liebmann and Smith, 1996*] and negative OLR anomalies are a good indicator of enhanced deep convective activity. Stippling denotes 95% statistical confidence based on a one-tail Student *t*-test.

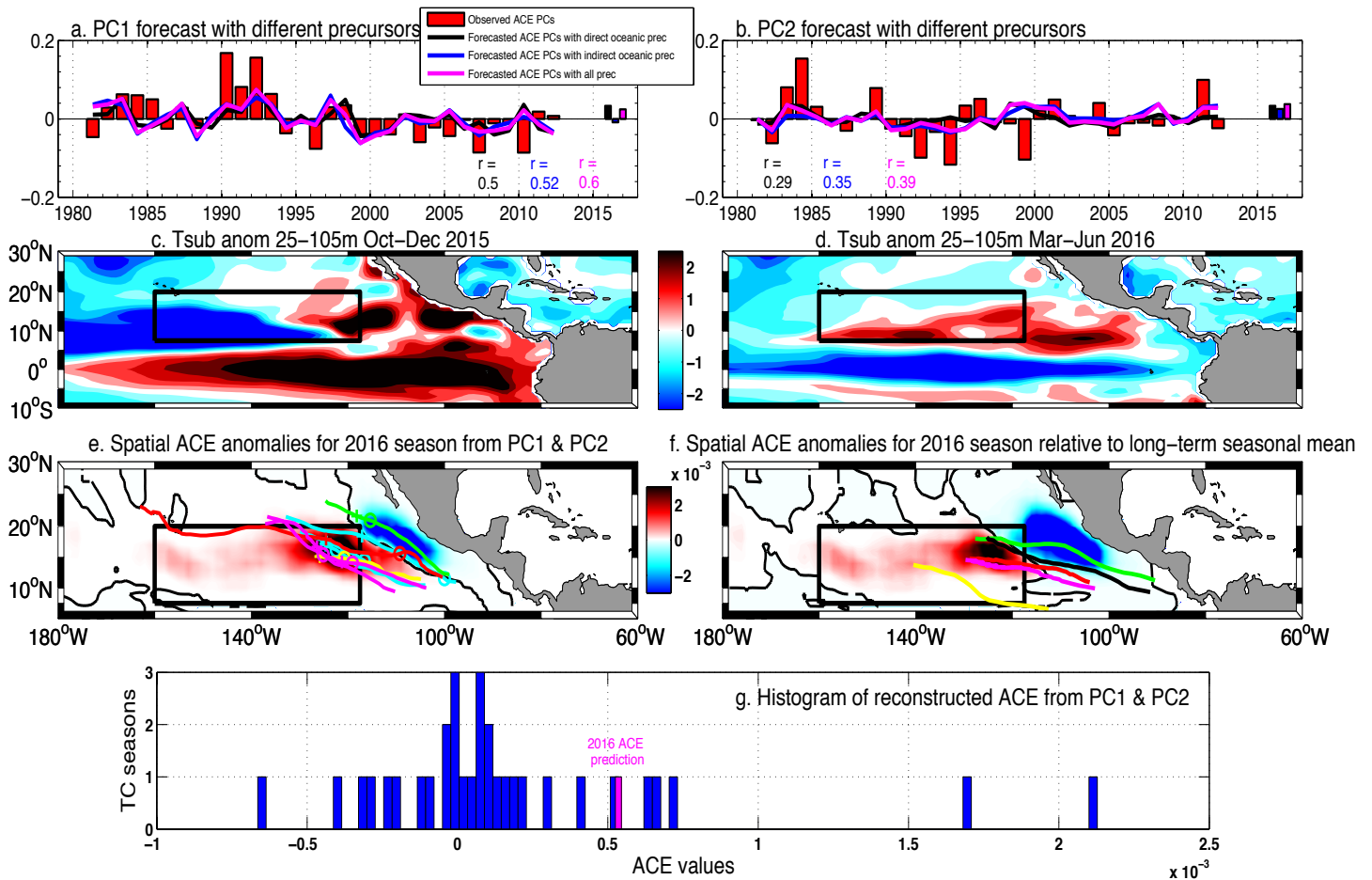


Figure S2. Observed (red bars) and forecasted values of PC1 in fall (panel a), PC2 in summer (panel b), with a multi-linear predictive model built using (1) only direct oceanic precursors (black dashed lines), (2) oceanic predictors of ENSO-induced atmospheric disturbances (blue dashed lines), without considering the wintertime intraseasonal anomalies of surface windstress in the Western Pacific (such as in Fig. 4); (3) using both type of predictors (magenta plain lines). Correlations between observed and predicted time series are indicated in each panel with the corresponding coloured font. Coloured bars on the right of panel a (b) represent the PC1 (PC2) prediction for the 2016 season using the corresponding predictors. Panel c (respectively d) shows anomalies of subsurface temperature (depth-averaged over 25–105m) in degrees celsius, averaged between October and December 2015 (respectively March–May 2016) illustrating the early discharge of subsurface heat into the Eastern Pacific hurricane region. Panel (e) shows the spatial reconstruction of ACE anomalies for the 2016

hurricane season (June- November) using the 2016 forecasts of both PC1 and PC2 with all predictors (i.e. projection of forecasted PC1 and PC2 onto the corresponding spatial EOF pattern). In panel (e), the coloured lines represent TC trajectories (excluding tropical depressions) that occurred in June and July 2016, cyan for Tropical Storms, green for Category 1, yellow for Category 2, red for Category 3, magenta for Category 4 and black for Category 5 hurricanes. The circles indicate the maximum wind intensification during each storm lifetime and the crosses stand for the location where the maximum wind speed is attained. Panel (f) shows the reconstructed ACE anomalies related to the long-term averaged (1980-2012) seasonal anomalies. In panel (f), the coloured lines represent the average track over the period 1980-2012 for each category of hurricanes that lasted more than 20 days between their maximum intensification and when their maximum wind speed is attained. Panel (g) shows the reconstructed seasonal values of ACE from PC1 and PC2 (1980-2012) and the predicted 2016 ACE seasonal value (magenta bar) averaged in the black box, as delineated in panel (c-f).